



Prediction of the Geometry of Low-Spin Iron(II) Complexes Using a Modified Concept of Partial Quadrupole Splitting (PQS): Advantages and Limitations

YAN Z. VOLOSHIN¹, ERNEST V. POLSHIN² and
ALEXANDER Y. NAZARENKO³

¹Karpov Institute of Physical Chemistry, 10, Vorontsovo pole Str., 103064 Moscow, Russia; e-mail: voloshin@cc.nifhi.ac.ru

²Institute of Geochemistry, Mineralogy and Ore Formation, 34, Palladina Ave, 252149 Kiev, Ukraine

³Department of Chemistry, State University of New York, College at Buffalo 1300 Elmwood Ave, Buffalo, NY 14222-1095, USA; e-mail: nazareay@bscmail.buffalostate.edu

Abstract. The advantages and limitations of the “absolute” PQS concept as well as examples of successful prediction of iron(II) clathrochelate geometry are discussed.

1. Introduction

Quadrupole splittings (QS) in Mossbauer spectra provide valuable information about the structure of low-spin iron(II) complexes. A very simple concept of partial quadrupole splitting (PQS) was developed [1, 2] in order to explain the peculiarities of QS in various compounds. For example, the substitution of one or two ligands B in an octahedral low-spin iron complex FeB_6 (QS = 0) results in the following QS values:

$$\begin{aligned} \text{QS} &= 2(\text{PQS}_A - \text{PQS}_B) && \text{FeAB}_5, \\ \text{QS} &= 4(\text{PQS}_A - \text{PQS}_B) && \textit{trans}\text{-FeA}_2\text{B}_4, \\ \text{QS} &= -2(\text{PQS}_A - \text{PQS}_B) && \textit{cis}\text{-FeA}_2\text{B}_4. \end{aligned} \quad (1)$$

In these cases QS is a function of the difference between PQS_A and PQS_B . Therefore, the absolute value of PQS cannot be calculated from the experimental QS value using these equations, and the relative PQS values depend on the choice of the reference value.

Contrary to the octahedral geometry, the trigonal prismatic (TP) environment of some iron(II) complexes provides a unique opportunity to obtain the QS of a complex with all donor groups being exactly the same. Therefore, the resulting PQS are “absolute”. We have reported an attempt to find the PQS absolute values

from X-ray and Mössbauer data for distorted TP low-spin iron(II) complexes [3]. Here we discuss the advantages and limitations of this approach.

2. Modified PQS concept

The degree of distortion of the iron(II) coordination polyhedron can be characterized by the angle φ , which varies from 0° (TP) to 60° (trigonal antiprism, TAP). The sign of QS changes with φ value in the series of complexes (Figure 1). In low-spin iron(II) complexes the three lowest d -orbitals are fully occupied (for octahedral complexes these are t_{2g} -orbitals). In the case of trigonal distortion, the t_{2g} -level splits into a_1 and e_1 . The value of such splitting, with allowance for the insignificant contribution of π -binding, has been calculated for macrobicyclic tris-diimine

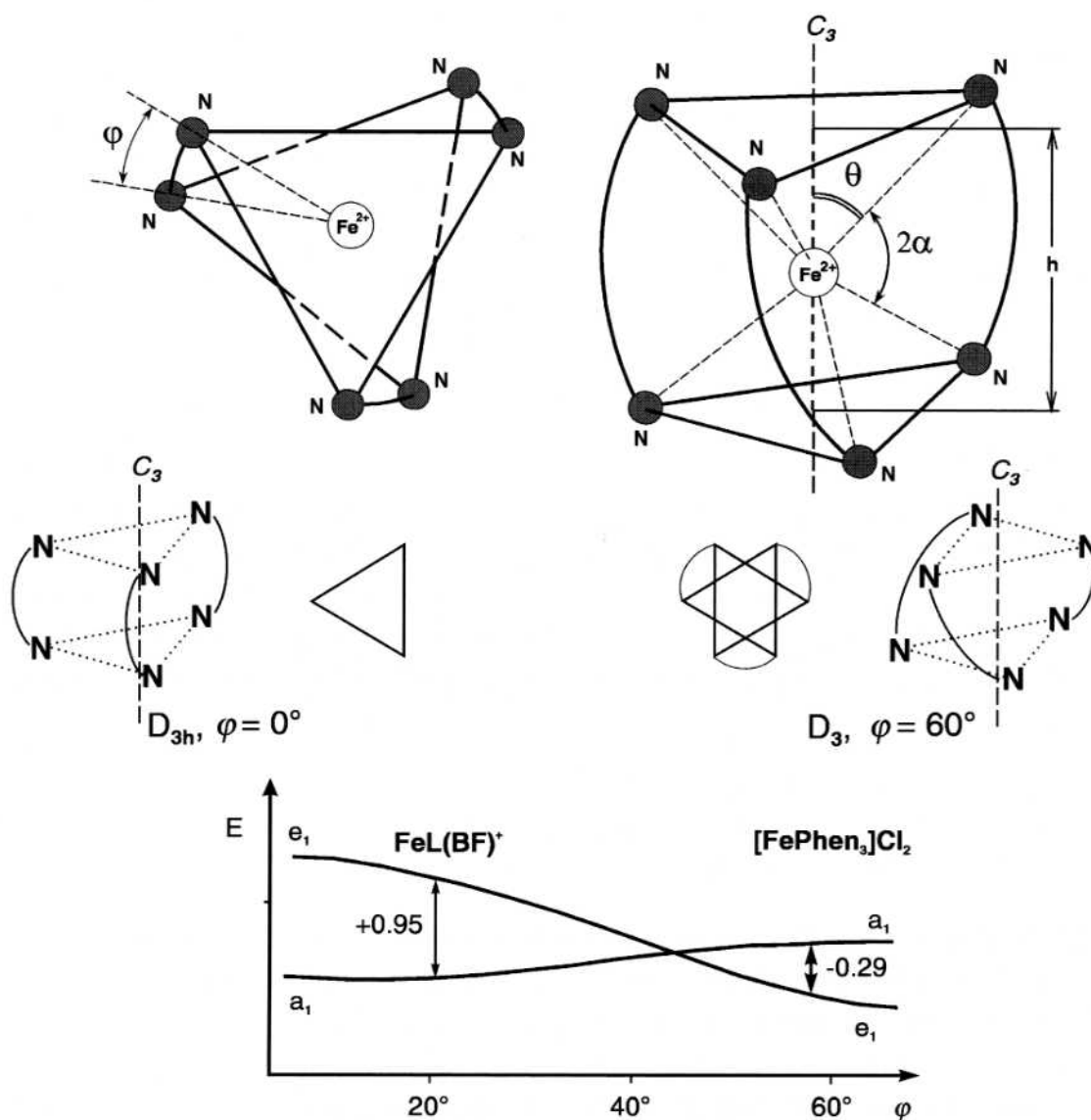


Figure 1. Distorted trigonal-prismatic FeN_6 coordination (the projection along the threefold axis and the side view, *top*) and t_{2g} -level splitting value *versus* coordination polyhedron distortion angle φ (*bottom*).

complexes [4]. At $\varphi = 60^\circ$ these complexes have the D_3 symmetry instead of O_h , which results in the non-zero value of splitting. With decrease of φ the splitting goes down to zero ($\varphi = 40\text{--}50^\circ$), after which an inversion of the levels takes place, and the splitting increases again (Figure 1). The splitting of the t_{2g} -levels and the absolute value of QS are parallel [5]. The sign of QS (obtained from ^{57}Fe Mössbauer experiments in magnetic field) is negative for the tris-phenanthroline complex ($\varphi = 56^\circ$) and positive for $\text{FePcc}(\text{BF})^+$ clathrochelate ($\varphi = 22^\circ$) [6]. When the geometry of the coordination polyhedron is close to TP, QS is large and positive ($\sim 1 \text{ mm s}^{-1}$). In complexes with TAP geometry QS is small and negative.

The QS for ^{57}Fe can be expressed as

$$\text{QS} = \frac{1}{2}e^2qQ(1 + \eta^2/3)^{1/2}, \quad (2)$$

where $q = V_{zz}/e$, $\eta = (V_{xx} - V_{yy})/V_{zz}$, and V are the components of the electric field gradient tensor [1]. We use two of Bancroft's assumptions from [1]:

(1) QS can be regarded as a sum of independent contributions, one from each ligand, and

(2) PQS's are constants for a given electronic state.

Two other assumptions were modified [3]:

(3) the structure of a distorted TP complex is determined by the bite angle 2α and the twist angle φ (Figure 1), and

(4) the z axis corresponds to the C_3 symmetry axis.

From symmetry reasons it is clear that $V_{xx} = V_{yy}$ and $\eta = 0$. Applying the same approximation as in the octahedral case, QS can be expressed as

$$\text{QS} = 6(3 \cos^2 \theta - 1) \cdot \text{PQS}, \quad \text{or} \quad \text{QS} = f \cdot \text{PQS}, \quad (3)$$

where f is a function of iron atom arrangement geometry and θ is the angle between the z axis and the Fe-N bond. For a given bidentate ligand, the θ value is a function of both bite angle α and distortion angle φ . Simple calculations give the following expression:

$$f = 12 - 18 \frac{\cos^2 \alpha}{\cos^2(\varphi/2)}. \quad (4)$$

For example, for an octahedron $\alpha = 45^\circ$, $\varphi = 60^\circ$, and $\text{QS} = f \cdot \text{PQS} = 0$. Using the available structural data for iron complexes and experimental QS values from the Mössbauer spectra (Table I), one can calculate the corresponding PQS values for each ligand (Table II). For all angles α the coefficient f has a negative sign in the case of pseudo-octahedral iron atom arrangement ($\varphi = 50\text{--}60^\circ$). For a TP iron atom the f values are comparatively high and positive. The effect of cross-linking groups on QS is much lower due to the significantly larger distance from the iron atom. Nevertheless, it can be described using the PQS treatment. The capping groups are located directly on the z axis of the complex; the contribution of each of these groups is $\Delta V_{zz} = (3 \cos^2 \theta - 1)z/r^3 = 2z/r^3$, where z is the

Table I. The Fe–N bond lengths a , base spacings h (Å), bite α and twist φ angles (deg), QS and PQS (mm/s), f values (calculated from Equation (4)) for macrobicyclic iron complexes

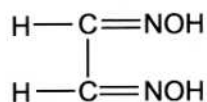
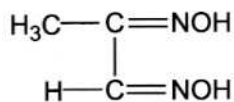
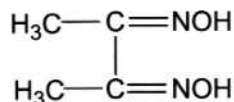
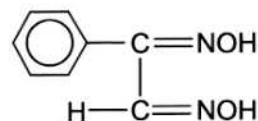
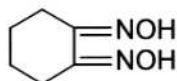
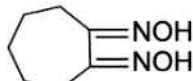
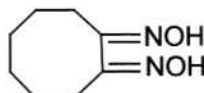
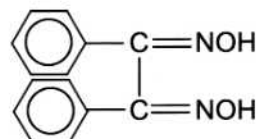
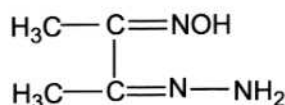
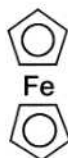
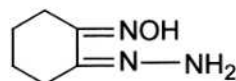
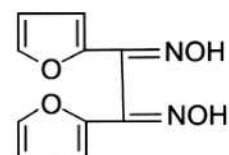
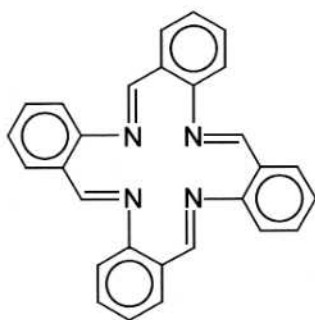
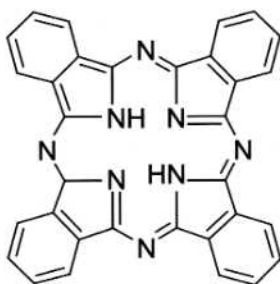
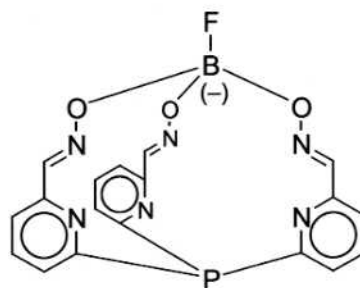
Compound ^a	a	h	α	φ	QS ^b	f	$f \cdot$ PQS	QS – $f \cdot$ PQS	Ref.
FePhm ₃ (BC ₆ H ₅) ₂ · BF ₃	1.91	2.34	39.2	21.8	(+0.48)	0.79	0.40	+0.1	[7]
FeBd ₃ (BF) ₂ · 5CHCl ₃	1.91	2.29	39.3	29.3	(+0.28)	0.49	0.25	+0.0	[8]
FeFd ₃ (BC ₆ H ₅) ₂ · 1/4CHCl ₃	1.91	2.31	39.2	26.4	0.0	0.60	0.30	–0.3	[9]
FeGx ₃ (BOH) ₂ · 3H ₂ O	1.91	2.33	39.1	23.4	(+0.50)	0.70	0.35	+0.15	[10]
FeGx ₃ (BC ₆ H ₅) ₂ · 2CHCl ₃	1.915	2.35	38.9	20.2	(+0.50)	0.75	0.38	+0.1	[11]
FeDm ₃ (BF) ₂ · C ₆ H ₆	1.91	2.40	39.0	21.2	(+0.67)	0.71	0.36	+0.3	[12]
FeGm ₃ (Bn–C ₄ H ₉) ₂	1.92	2.39	38.6	10.9	(+0.84)	0.90	0.45	+0.4	[9]
[FePcc(BF)] ⁺	1.91		39.5	21.8	+0.95	0.90	0.45	+0.4	[13]
FeNx ₃ (BFc) ₂ · 2CCl ₄	1.90	2.38	39.3	9.5	(+0.72 (Fe ²⁺)) (+2.36 (Fc))	1.16	0.58	+0.15	[14]
FeNx ₃ (Bn–C ₄ H ₉) ₂	1.91	2.34	39.1	20.3	(+0.58)	0.81	0.41	+0.2	[15]
FeGx ₃ (Bn–C ₃ H ₇) ₂	1.90	2.31	38.8	21.8	(+0.37)	0.66	0.33	0	[16]
FeOx ₃ (Bn–C ₄ H ₉) ₂ · CCl ₄	1.90	2.34	39.2	25.2	(+0.33)	0.65	0.33	0	[16]
[FeCXO ₃ (BC ₆ H ₅)(HCOC ₂ H ₅) ₃](BF ₄) · 1/2C ₆ H ₆	1.90	2.37	38.7	10.8	(+0.38)	0.94	0.47	–0.1	[17]
	1.91								
[FeCXO ₃ (BC ₆ H ₅)(HCOC ₂ H ₅) ₃](BF ₄)	1.90	2.34	38.8	18.2	(+0.34)	0.79	0.40	–0.1	[17]
	1.93								
FeNx ₃ (BAllyl) ₂	1.90	2.36	38.9	13.8	(+0.74)	0.94	0.47	+0.3	[18]
				17.0		0.85	0.43	+0.3	
FeNx ₃ (BHd) ₂ (at 298 K)	1.91	2.37	38.9	10	(+0.68)	1.01	0.51	+0.2	[18]
		2.35		18		0.83	0.42	+0.3	
FeDm ₃ (BAllyl) ₂	1.90	2.35	38.4	8.1	(+0.69)	0.89	0.45	+0.25	[18]
FeNx ₃ (BC ₆ H ₃ (OCH ₃) ₂) ₂ · CHCl ₃	1.90	2.35	39.1	17.8	(+0.84)	0.89	0.45	+0.4	[19]

Table I. (Continued)

FeNx ₃ (BC≡C-C ₆ H ₅) ₂ · C ₆ H ₅ CH ₃	1.90	2.36	38.7	11.5	(+)0.67	0.93	0.47	+0.2	[19]
Fe(Cl ₂ Gm) ₃ (BC ₆ H ₅) ₂	1.91	2.35	39.1	20.0		0.82	0.41	+0.3	
Fe(Cl ₂ Gm) ₃ (Bn-C ₄ H ₉) ₂	1.90	2.39	39.0	5.4	0.68	1.11	0.55	+0.1	[20]
Fe(Cl ₂ Gm) ₃ (BF) ₂ · 2THF	1.90	2.38	39.1	16.1	0.62	0.94	0.47	+0.15	[21]
Fe((C ₆ H ₅ O) ₂ Gm) ₃ (Bn-C ₄ H ₉) ₂	1.91	2.36	39.0	17.1	0.64	0.88	0.44	+0.2	[21]
Fe((CH ₃ S) ₂ Gm) ₃ (BC ₆ H ₅) ₂ · THF	1.91	2.32	39.3	25.2	0.52	0.84	0.42	+0.1	[21]
Fe((C ₆ H ₅ S) ₂ Gm) ₃ (BC ₆ H ₅) ₂	1.91	2.33	39.5	25.3	0.29	0.68	0.34	+0.05	[21]
Fe((n-C ₄ H ₉ NH) ₂ Gm) ₂ (Cl ₂ Gm)(BC ₆ H ₅) ₂	1.92	2.33	39.5	25.6	0.25	0.73	0.37	+0.1	[20]
	1.91	2.30	39.0	27.3	0.69	0.65	0.33	+0.4	[21]
	1.91	2.30	39.0	29.2	0.69	0.55	0.28	+0.4	
FeBd ₂ (Cl ₂ Gm)(BF) ₂ · 2C ₆ H ₆	1.91	2.33	39.3	24.8	0.62	0.70	0.35	+0.3	[22]
FeBd ₂ ((C ₂ H ₅) ₂ N)ClGm)(BF) ₂ · C ₆ H ₆	1.91	2.31	39.3	26.6	0.31	0.62	0.31	0.0	[22]
FeBd ₂ ((CH ₃ S) ₂ Gm)(BF) ₂	1.90	2.31	39.3	25.8	0.36	0.66	0.33	0.0	[22]
FeNx ₃ (Sb(C ₂ H ₅) ₃) ₂	1.91	2.26	39.8	35.7	(-)0.27	0.27	0.14	-0.4	[19]
[FeNx ₃ (SnCl ₃) ₂] ²⁻	1.92	2.23	39.5	37.5	(-)0.19	0.04	0.02	-0.2	[23]

^a Ligand designations are shown in Scheme 1.

^b QS values were obtained at X-ray structure analysis temperatures.

Glyoxime,
H₂GmMethylglyoxime,
H₂MmDimethylglyoxime,
H₂DmPhenylglyoxime,
H₂PhmNioxime,
H₂NxHeptoxime,
H₂GxOctoxime,
H₂Ox α -Benzylidioxime,
H₂BdDiacetylmonooxime
hydrazone,
DXOH**Fc**1,2-cyclohexanedione-
monooxime hydrazone,
CXOH α -Furyldioxime,
H₂Fd**TAAB****Pc****Iz****Pcc(BF)**

Scheme 1.

charge on the capping atom. The overall QS value increases with q . For iron trisdioximates the range of α usually observed is narrow ($38\text{--}40^\circ$), and the QS value is a function of only φ angle and the effect of capping groups.

It is useful to compare the PQS values calculated by Bancroft and ours (Table II). The modified PQS scale can be obtained from Bancroft's scale by adding 1.3 mm s^{-1} . This number was obtained by comparing the PQS values for nioxime, phenanthroline and bipyridine complexes in both scales. All PQS values obtained

Table II. PQS values for some ligands and quadrupole splittings (mm s^{-1}) for iron(II) complexes used for PQS calculations

Compound ^a	Δ (calc.)	Δ (exp.)	Bancroft scale	PQS ^b	Σ ^c	Ref.
phen			-0.95	0.35	0.35	[3]
dipy			-0.85	0.45	0.45	[3]
HDm ⁻ , HNx ⁻			-0.92	0.38	0.38	[3]
Fe(HNx) ₂ Py ₂	1.76	1.79				[24, 25]
Fe(HDm) ₂ Py ₂	1.76	1.74				[26]
HBd ⁻			-0.97		0.33	[3]
Fe(HBd) ₂ Py ₂	1.96	1.97				[26]
Fe(HNx) ₂ (CNC ₆ H ₁₁) ₂	0.92	0.94				[27]
Macrocyclic			-0.86		0.44	[28]
TAAB			-0.62		0.68	[28]
[Fe(TAAB)(CH ₃ CN) ₂](BF ₄) ₂	0.76	0.82				[29]
NH ₃			-0.52		0.78	[1]
Fe(HNx) ₂ (NH ₃) ₂	1.60	1.72				[24, 25]
Py, <i>n</i> -C ₄ H ₉ NH ₂			-0.48		0.82	[3]
Fe(HNx) ₂ (<i>n</i> -C ₄ H ₉ NH ₂) ₂	1.76	1.83				[24, 25]
Iz			-0.53		0.77	[3]
Fe(HNx) ₂ (Iz) ₂	1.56	1.38				[24, 25]
CN ⁻			-0.84		0.46	[1]
Fe(HNx) ₂ (CN)(Iz)	0.94	0.93				[24, 25]
Pc			-0.98		0.32	[3]
FePc(BuNH ₂) ₂	2.0	1.94				[24, 25]
K ₂ FePc(Iz) ₂	1.80	1.75				[24, 25]
FePc(CN) ₂	0.56	0.56				[24, 25]
FePc(Py) ₂	2.0	1.97				[24, 25]
NO			+0.04		1.34	[1]

^a Ligand designations are shown in Scheme 1. ^b Calculated from Equation (4). ^c Σ is calculated from Bancroft PQS by addition of 1.3 mm s^{-1} .

are positive, in contrast to Bancroft scale with negative PQS for all ligands except NO. It is clear that the nature of PQS is rather different from the pure electrostatic effect of the charge of ligand atoms. The reason of a positive PQS value is a decrease in electron density around the iron atom ($r < 0.5 \text{ \AA}$) which was observed by direct electron density measurements in sodium nitroprusside, $[\text{Co}(\text{CN})_6]^{3-}$ and $[\text{Co}(\text{NH}_3)_6]^{3+}$ [30, 31]. The highest electron density decrease has been observed along the Fe-NO and Co-NH₃ bonds, and the lowest one is along the Fe-CN and Co-CN bonds. These data correlate with the magnitude of PQS for NO, NH₃ and CN (Table II).

3. Successful predictions of iron(II) clathrochelates geometry

The QS values in the ^{57}Fe Mössbauer spectra for clathrochelate tin-containing complexes [32] are small; they change in the dioxime series in an order which differs greatly from that observed for boron-containing compounds. The temperature dependence of QS for the $[\text{FeN}_x_3(\text{SnCl}_3)_2]^{2-}$ dianion shows an increase in splitting as temperature decreases. This trend is the same as in the non-macrocyclic $[\text{Fe}(\text{H}_2\text{N}_x)_3]\text{SO}_4$ complex [5] (TAP geometry) and opposite to boron-containing iron(II) dioximates (TP).

This allowed us to suggest a negative sign of QS and TAP geometry with distortion angles $\varphi \sim 40\text{--}55^\circ$ in the case of the clathrochelate tin-containing dianions. The minimal distortion angle value ($\sim 40^\circ$) has been predicted for the nioxime complex with the lowest QS value [32].

Two years later, we determined the structure of clathrochelate $[\text{FeN}_x_3(\text{SnCl}_3)_2]^{2-}$ dianion by X-ray analysis [23]. The central iron atom of this dianion has a coordination polyhedron intermediate between TAP and TP with $\varphi = 37.5^\circ$. This distortion angle is somewhat lower than the value predicted from the QS value.

This novel version of PQS can be applied successfully to the prediction of geometry of the hexadecyl- and allylboronate trisdioximates [18], ferrocenylboronic clathrochelates [14], and macrobicyclic trisoximehydrazonates [17]. A good coincidence between QS_{exp} and QS_{calcd} has been observed even in the case of non-symmetrical $\text{FeBd}_2((\text{N}(\text{C}_2\text{H}_5)_2)\text{ClGm})(\text{BF})_2$ and $\text{FeBd}_2((\text{CH}_3\text{S})_2\text{Gm})(\text{BF})_2$ complexes (Table I).

4. QS in tetragonal diimine iron complexes

The modified PQS model is not limited to TP geometry. An interesting example of using the absolute PQS model is the case of complexes with two bidentate ligands in the equatorial plane and two monodentate ligands in axial positions. In many compounds $\alpha \neq 45^\circ$ and $V_{XX} \neq V_{YY}$, $\eta > 0$. This phenomenon causes a slight increase in QS. But if $\text{PQS}_{\text{EQ}} \rightarrow \text{PQS}_{\text{AX}}$, then $V_{ZZ} = 4(\text{PQS}_{\text{AX}} - \text{PQS}_{\text{EQ}}) \rightarrow 0$; the distortion in the xy plane becomes most important and causes the reorientation of the axes. In this case

$$V_{ZZ} = 4(3 \cos^2 \theta - 1)\text{PQS}_{\text{EQ}} - 2\text{PQS}_{\text{AX}} = F \cdot \text{PQS}_{\text{EQ}} - 2\text{PQS}_{\text{AX}}, \quad (5)$$

where $F = 4(3 \sin^2 \alpha - 1)$ and 2α is the bite angle. Furthermore, if $\text{PQS}_{\text{AX}} = \text{PQS}_{\text{EQ}}$, then $V_{ZZ} = -6 \cos(2\alpha)\text{PQS}$ and $(1 + \eta^2/3)^{1/2} = 1.16$. For common bite angles of α -diimine ligands ($38\text{--}41^\circ$) QS is between -1.0 PQS and -1.7 PQS. Even a slight displacement of equatorial donor atoms from the xy plane can increase the splitting because the corresponding θ angles are near the "magic" angle.

Compounds with four diimine nitrogen donor atoms in equatorial positions and with two cyano-groups in axial ones are examples of such complexes. The

PQS's of both donor groups are very close (Table II) and equal to +0.46 (CN) and +0.38 mm s^{-1} (HNx^-). Using the approach described above, the QS of such compounds can be estimated as -0.7 – 0.8 mm s^{-1} . This result is in a good agreement with experimental data for $[\text{Fe}(\text{HNx})_2(\text{CN})_2]$ (0.80 mm s^{-1}), $[\text{Fe}(1,3,8,10\text{-}[14]\text{tetraeneN}_4)(\text{CN})_2]$ (1.09 mm s^{-1}) and $[\text{Fe}(1,3,8\text{-}[14]\text{trieneN}_4)(\text{CN})_2]$ (0.90 mm s^{-1}) complexes. All these cases could not be described by the octahedral *trans*- FeA_2B_4 model, which predicts QS of 0.2 – 0.3 mm s^{-1} .

5. Limitations

The applicability of the major concepts of the PQS model to iron(II) complexes is associated with an axial symmetry of the electron density distribution (EDD) about the iron atom. Such symmetry is important to establish the correlation between QS and the geometry of the coordination environment. In the case of octahedral complexes, this assumption has been confirmed by the results of calculations and by the experimental measurements of the EDD. For example, the deformation electron density (DED) map for sodium nitroprusside (FeB_5A geometry) demonstrates a nearly axial charge distribution around the iron atom in the equatorial plane [30].

However, we have observed an example of deviation from DED axial symmetry even in the case of the formally C_3 -symmetrical complex. A single crystal of $\text{FeDm}_3(\text{BF})_2 \cdot \text{C}_6\text{H}_6$ complex has been studied by X-ray diffraction at 138, 208, and 291 K and by ^{57}Fe Mössbauer spectroscopy in the temperature range from 135 to 290 K [12]. The molecular geometry of the $\text{FeDm}_3(\text{BF})_2$ clathrochelate (Figure 2) does not substantially change in the temperature range under study. The complex has pseudo- C_3 symmetry, and φ is equal to 21.2° . The iron atom is displaced from the center of the N_6 coordination polyhedron along the threefold pseudoaxis by 0.034, 0.026 and 0.023 Å at 138, 208 and 291 K, respectively.

The presence of the local C_3 symmetry in the $\text{FeDm}_3(\text{BF})_2$ molecule implies that the EDD is axially symmetrical. The DED for the $\text{FeDm}_3(\text{BF})_2$ molecule has been examined by X-ray diffraction [12]. The maxima of the DED in the vicinity of the metal ion correspond to the partial or complete localization of the complex molecular orbitals (MO) on the metal ion. Actually, the maxima of the DED were found in the vicinity of the iron ion in the DED sections (Figure 2) passing through the iron, boron, and fluoride atoms (section A) and in the equatorial plane (section B). The accumulation of the DED along the three-fold axis and in the equatorial plane corresponds to the a_1 -MO and the e_1 -MO, respectively. However, unlike the expected axial symmetry of the DED distribution, it is characterized (see the section B) only by the symmetry plane passing through the C(1), C(1'), and iron atoms (the local symmetry C_s). Therefore, in spite of the equivalence of the α -dioximate fragments, the interaction of the iron(II) ion with the macrobicyclic ligand (according to the DED map) is anisotropic. As a result, the experimental QS value ($\sim 0.7 \text{ mm s}^{-1}$) for $\text{FeDm}_3(\text{BF})_2 \cdot \text{C}_6\text{H}_6$ complex is higher than the value

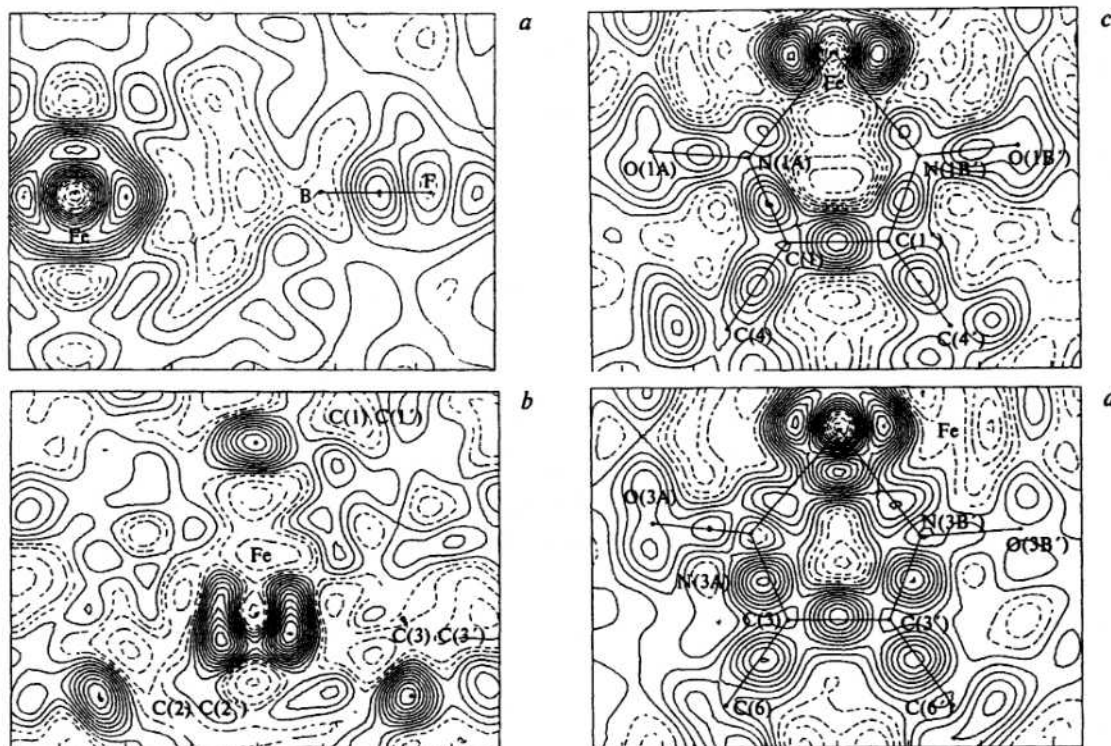
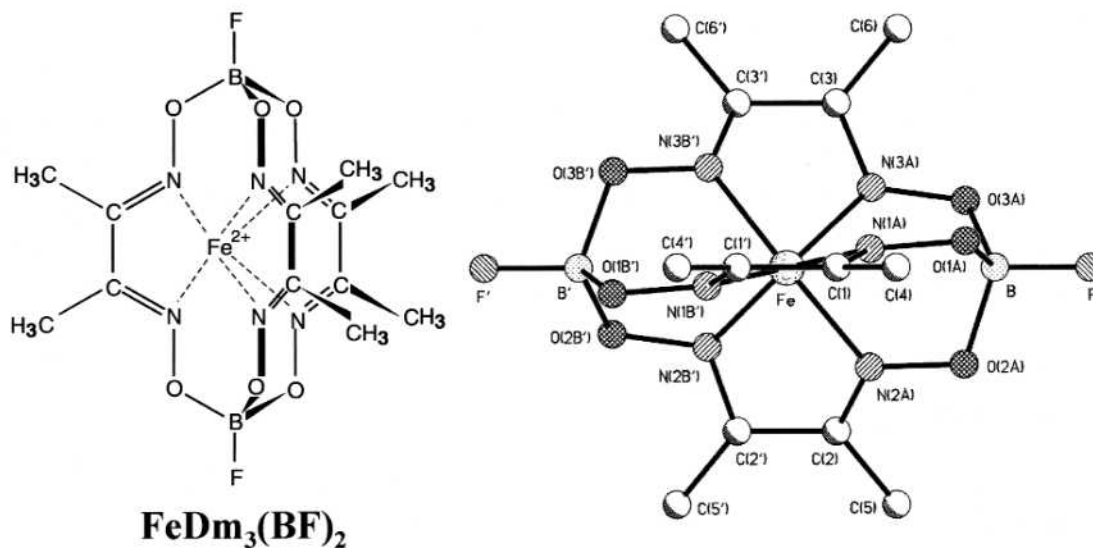


Figure 2. General view of $\text{FeDm}_3(\text{BF})_2$ molecule and the deformation electron density maps passing through the Fe, B, and F atoms (a), through the midpoints of the C(1)–C(1'), C(2)–C(2'), and C(3)–C(3') bonds (b), and in the mean planes of the chelate rings (c) and (d) [12].

calculated from the PQS model (0.38 mm s^{-1}). In this case one of the major assumptions of the PQS concept, regarding the equivalence of the PQS values for donor atoms, is inapplicable. Thus, the displacement of the iron ion from the center of the coordination polyhedron along the threefold axis and the axial asymmetry of EDD about iron(II) ion leads to a significant increase in the electric field gradient on the iron nucleus.

6. Conclusion

The PQS values obtained have a real physical meaning and reflect the EDD in the molecule, allowing us to explain QS for a great number of iron coordination compounds with different geometry. These values make it possible to predict the structure of new compounds from the "structure-vs.-quadrupole splitting" type of correlation dependence. Taking into account the peculiarities of ligands (e.g., capping groups, substituents, protonation-deprotonation processes) may noticeably change the QS. The main reason for deviations from the proposed PQS model is the EDD asymmetry caused by non-equivalence of donor atoms.

References

1. (a) Bancroft, G. M., *Coord. Chem. Rev.* **11** (1973), 247; (b) Bancroft, G. M., *Mössbauer Spectroscopy – An Introduction for Inorganic Chemists and Geochemists*, McGraw-Hill, New York, 1973.
2. Parish, R. V., *Structure and Bonding in Tin Compounds. Mössbauer Spectroscopy Applied to Inorganic Chemistry*, Vol. 1, Plenum Press, New York, 1984.
3. Nazarenko, A. Y., Polshin, E. V. and Voloshin, Y. Z., *Mendeleev Commun* **45** (1993).
4. Larsen, E., La Mar, G. N., Wagner, E. B. and Holm, R. H., *Inorg. Chem.* **11** (1972), 2652.
5. Voloshin, Y. Z., Kostromina, N. A. and Nazarenko, A. V., *Inorg. Chim. Acta* **170** (1990), 181.
6. Reiff, W. M., *J. Am. Chem. Soc.* **95** (1973), 3048.
7. Zavodnik, V. E., Belsky, V. K., Voloshin, Y. Z. and Varzatskii, O. A., *J. Coord. Chem.* **28** (1993), 97.
8. Lindeman, S. V., Struchkov, Y. T. and Voloshin, Y. Z., *Inorg. Chim. Acta* **184** (1991), 107.
9. Lindeman, S. V., Struchkov, Y. T. and Voloshin, Y. Z., *Polish J. Chem.* **67** (1993), 1575.
10. Voloshin, Y. Z., Lindeman, S. V. and Struchkov, Y. T., *Koord. Khim.* **16** (1990), 1367.
11. Zavodnik, V. E., Belsky, V. K. and Voloshin, Y. Z., *Polish J. Chem.* **67** (1993), 1567.
12. Vorontsov, I. I., Lysenko, K. A., Potekhin, K. A., Antipin, M. Y., Voloshin, Y. Z., Polshin, E. V. and Varzatskii, O. A., *Rus. Chem. Bull. Int. Ed.* **49** (2000), 2018.
13. Churchill, M. R. and Reis, A. H., *Inorg. Chem.* **11** (1972), 2299.
14. Voloshin, Y. Z., Kron, T. E., Belsky, V. K., Zavodnik, V. E., Maletin, Y. A. and Kozachkov, S. G., *J. Organomet. Chem.* **536/537** (1997), 207.
15. Kubow, S. A., Takeuchi, K. J., Grzybowski, J. J., Jircitano, A. J. and Goedkin, V. L., *Inorg. Chim. Acta* **241** (1996), 21.
16. Voloshin, Y. Z., Terekhova, M. I., Noskov, Y. G., Zavodnik, V. E. and Belsky, V. K., *Anal. Quim. Int. Ed.* **94** (1998), 142.
17. Voloshin, Y. Z., Stash, A. I., Varzatskii, O. A., Belsky, V. K., Maletin, Y. A. and Strizhakova, N. G., *Inorg. Chim. Acta* **284** (1999), 180.
18. Voloshin, Y. Z., Varzatskii, O. A., Stash, A. I., Belsky, V. K., Bubnov, Y. N., Vorontsov, I. I., Potekhin, K. A., Antipin, M. Yu. and Polshin, E. V., *Polyhedron* **20** (2001), 2721.
19. Voloshin, Y. Z., Zavodnik, V. E. and Vorontsov, I. I., unpublished results.
20. Voloshin, Y. Z., Varzatskii, O. A., Palchik, A. V., Stash, A. I. and Belsky, V. K., *New J. Chem.* **23** (1999), 355.
21. Voloshin, Y. Z., Varzatskii, O. A., Kron, T. E., Belsky, V. K., Zavodnik, V. E., Strizhakova, N. G. and Palchik, A. V., *Inorg. Chem.* **39** (2000), 1907.
22. Voloshin, Y. Z., Zavodnik, V. E., Varzatskii, O. A., Belsky, V. K., Palchik, A. V., Strizhakova, N. G., Vorontsov, I. I. and Antipin, M. Yu., 2001, in press.
23. Lindeman, S. V., Struchkov, Y. T. and Voloshin, Y. Z., *J. Coord. Chem.* **28** (1993), 319.

24. Dale, B. W., Williams, R. J. R., Edwards, P. R. and Jonson, C. E., *Trans. Farad. Soc.* **64** (1968), 620.
25. Dale, B. W., Williams, R. J. R., Edwards, P. R. and Jonson, C. E., *Trans. Farad. Soc.* **64** (1968), 3011.
26. Stukan, R. A., Turta, K. I., Ablov, A. V., Zubareva, V. I. and Goldman, A. M., *Zh. Neorg. Khim.* **21** (1976), 286 [*Russ. J. Inorg. Chem.* **21** (1976), 155].
27. Turta, K. I., Bulgak, I. I., Starysh, M. P., Stukan, R. A. and Batyr, D. G., *Koord. Khim.* **6** (1980), 1041 [*Sov. J. Coord. Chem. (Engl. Trans.)* **6** (1980), 520].
28. Dabrowiak, J. C., Merrell, P. H., Stone, J. A. and Busch, D. H., *J. Am. Chem. Soc.* **95** (1973), 6613.
29. Polshin, E. V. and Rybak-Akimova, E., personal communication.
30. Antipin, M. Y., Tsirelson, V. G., Flugge, M. P., Struchkov, Y. T. and Ozerov, R. P., *Koord. Khim.* **13** (1987), 121 [*Sov. J. Coord. Chem. (Engl. Trans.)* **13** (1987), 67].
31. Iwata, M. and Saito, Y., *Acta Crystallogr. B* **29** (1973), 822.
32. Voloshin, Y. Z., Kostromina, N. A., Nazarenko, A. Y. and Polshin, E. V., *Inorg. Chim. Acta* **185** (1991), 83.